Ultranarrow Luminescence Lines from Single Quantum Dots

M. Grundmann,* J. Christen,† N. N. Ledentsov,‡ J. Böhrer, and D. Bimberg
Institut für Festkörperphysik, Technische Universität Berlin, Hardenbergstrasse 36, D-10623 Berlin, Germany

S. S. Ruvimov,‡ P. Werner, U. Richter,§ U. Gösele, and J. Heydenreich
Max-Planck-Institut für Mikrostrukturphysik, Weinberg 2, D-06120 Halle, Germany

V. M. Ustinov, A. Yu. Egorov, A. E. Zhukov, P. S. Kop'ev, and Zh. I. Alferov
A. F. Ioffe Physical-Technical Institute, Politekhnicheskaya 26, 194021 St. Petersburg, Russia
(Received 23 May 1994)

We report ultranarrow (< 0.15 meV) cathodoluminescence lines originating from single InAs quantum dots in a GaAs matrix for temperatures up to 50 K, directly proving their δ-function-like density of electronic states. The quantum dots have been prepared by molecular beam epitaxy utilizing a strain-induced self-organizing mechanism. A narrow dot size distribution of width 12 ± 1 nm is imaged by plan-view transmission electron microscopy. Cathodoluminescence images directly visualize individual dot positions and recombination from a *single* dot. A dense dot array ($\sim 10^{11}$ dots/cm^2) gives rise to a distinct absorption peak which almost coincides with the luminescence maximum.

PACS numbers: 73.20.Dx, 36.40.−c, 78.55.−m, 78.60.Hk

Semiconductor quantum dots (QD's) are expected to exhibit exciting new electronic and optical properties such as an atomiclike δ-function density of states (DOS) not found for three-, two-, and one-dimensional structures, and strongly increased exciton binding energies and oscillator strength [1–3]. Thus great effort is currently underway to fabricate nm-scale QD's.

Because of full quantization in all three dimensions the eigenspectrum of a *single* dot always consists of a *discrete* set of eigenenergies depending only on the number of atoms making up a dot. Variations of strain or shape lead to additional continuous variation of the eigenenergies from dot to dot. The finite carrier lifetime will introduce Lorentzian broadening $S(E)$ of finite width Γ. Thus, taking into account only ground-state transitions (the quantization effects in our dots are so high that only one electron level exists), the recombination spectrum R_N of N quantum dots is a series of sharp lines,

$$R_N(h\nu) = \sum_{n=1}^{N} S(h\nu - E_n). \quad (1)$$

This is especially valid for high temperatures where $k_B T \gg \Gamma$ and has to be experimentally verified in order to prove zero-dimensional DOS. No such *spectroscopic* confirmation for the existence of δ-function DOS in these structures is available in the literature so far. Size fluctuations between single dots will lead to a statistical distribution $\mathcal{P}(E)$ of the eigenenergies, characterized by a spectral width W. In the limit of a large number of dots, as, e.g., sampled by photoluminescence, the recombination spectrum of the *dot ensemble* R_∞ is given by the convolution of the single QD spectrum with the distribution function. Since $\Gamma \gg W$, the spectrum basically reflects the statistical fluctuations between dots,

$$R_\infty(h\nu) = \int S(h\nu - E)P(E)\,dE \sim P(h\nu). \quad (2)$$

The few spectra of nm-scale dot systems reported up to now represent the dot ensemble average R_∞, are usually several 10 meV broad (e.g., [4,5]), and cannot reflect the zero-dimensional character of the electronic properties. In this Letter we present for the first time direct evidence for a δ-function density of states of *single* nm-scale QD's, observed by cathodoluminescence (CL) imaging up to 50 K.

Several approaches for *in situ* fabrication of QD's were reported hitherto: formation of microcrystallites in a glass matrix [6], growth on stepped surfaces [7], formation of corrugated superlattices on self-organized microscopically ordered faceted surfaces [8], and strain-induced self-organized growth of QD's [4,5,9–13]. We employ the latter approach and fabricate structures consisting of a plane of InAs QD's inserted into a GaAs quantum well, confined by short period GaAs-$Al_{0.3}Ga_{0.7}As$ superlattices.

The samples are grown by elemental source molecular beam epitaxy (MBE) on GaAs(001) substrates. Growth rates are 0.8 μm/h for GaAs and 0.3 μm/h for InAs. Arsenic pressure was $(2-3) \times 10^{-6}$ torr. After oxide desorption, a 0.5-μm-thick GaAs buffer is grown at 600 °C, then 200 Å of the $Al_{0.3}Ga_{0.7}As$ is deposited, followed by a 2 nm/2 nm GaAs-$Al_{0.3}Ga_{0.7}As$ superlattice (5 periods), and a 7 nm GaAs layer. Then the substrate temperature is lowered to 450 °C and the desired amount of InAs is deposited. Afterward 5 nm of GaAs is grown at 450 °C, then the substrate temperature is increased to 600 °C, and a 2-nm-thick GaAs layer is grown. This layer is followed by a 2 nm/2 nm GaAs-$Al_{0.3}Ga_{0.7}As$ superlattice (5 periods) and 20 nm of $Al_{0.3}Ga_{0.7}As$; a 5 nm GaAs layer is grown on the top for surface protection. Reflection high-energy electron diffraction (RHEED) patterns are monitored during the

growth. Formation of dots starts after the deposition of a ~0.5-nm-thick InAs layer and leads to the transformation of a streaky RHEED pattern to a dashed one. Further InAs deposition results in well-developed diffraction spots typical for a three-dimensional growth mode. The average thickness t_{av} of InAs deposited is 0.6 and 1.2 nm, respectively.

Transmission electron microscopy (TEM) studies are carried out in a high voltage JEOL JEM1000 microscope operated at 1 MV. Photoluminescence (PL) is excited using the 632.8 nm line of a He-Ne laser and detected using a cooled germanium *p-i-n* photodetector. Excitation density is about 1 W/cm^2. Cathodoluminescence studies [14] are performed using low excitation voltage (3 kV and beam current (60 pA), ensuring high geometrical lateral resolution below 50 nm. Actual lateral resolution might be lowered by carrier diffusion. The luminescence is detected with a 512-channel infrared-intensified diode array. The spectral resolution is presently limited to 0.09 nm (0.15 meV at 880 nm). Calorimetric absorption spectroscopy (CAS) is carried out at $T = 500$ mK. Minimal detectable αd products are as low as 10^{-5} [15].

Figure 1 shows plan-view TEM images of the InAs QD's under two-beam bright field imaging conditions. Figures 1(a) and 1(b) correspond to an average thickness of InAs of $t_{av} = 0.6$ and 1.2 nm, respectively. When t_{av} is increased, the intensity of the dot-induced contrast and the areal density of dots increase from 3×10^{10} to 10^{11} dots/cm^2. For $t_{av} = 1.2$ nm dots have a predominantly pyramidal shape with a square base 12 ± 1 nm in width as derived from weak beam images. Their principal axes are close to the ⟨100⟩ directions. The height of the dots is 5 ± 1 nm estimated from cross-section TEM's. In the case of $t_{av} = 0.6$ nm, the size distribution is broader, and most dots are smaller in volume by a factor of about 4 and do not show a well defined crystallographic shape.

CAS and PL spectra of the structures are shown in Figs. 2(a)–2(d). The absorption due to the GaAs substrate (measured on the same samples with the dots etched off) has been subtracted from the CAS spectra. An intense luminescence line (FWHM = 60 meV) having a maximum shifted towards smaller photon energies in comparison to uniform InAs quantum wells [16,17] is observed. For the case of the $t_{av} = 1.2$ nm sample the maximum of emission almost perfectly coincides with the absorption peak. The absorption peak at 1.38 eV is due to the residual 2D layer (1.7 ML), as additionally evidenced by PL excitation spectroscopy [18]. In contrast to this, in the case of the $t_{av} = 0.6$ nm sample, a large shift between the dot PL maximum and the onset of the absorption is found. The absorption is actually due to the InAs wetting layer, which is slightly thinner (1.25 ML) than for the $t_{av} = 1.2$ nm sample; no absorption from the dots could be detected.

The PL peak position of the $t_{av} = 1.2$ nm InAs dots shifts as expected from the temperature dependence of the InAs and GaAs band gaps by about 80 meV between 2 K and room temperature. The intensity of emission remains nearly constant between 2 and 150 K and then drops with an activation energy of ~190 meV, indicating efficient

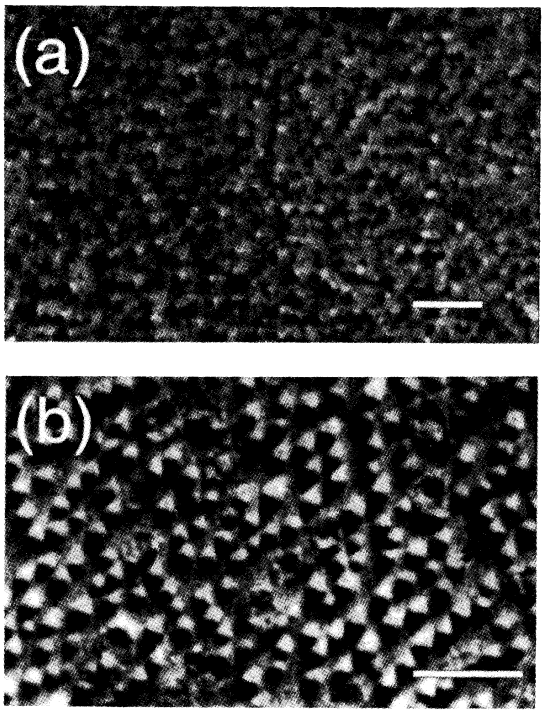

FIG. 1. Plan-view TEM images of InAs quantum dots in a GaAs matrix. Average thickness of InAs deposited is (a) $t_{av} = 0.6$ nm and (b) $t_{av} = 1.2$ nm. Markers represent 100 nm.

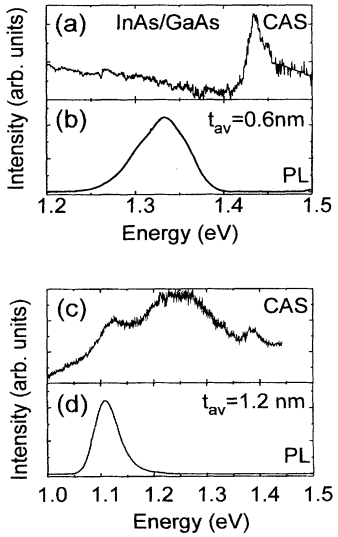

FIG. 2. CAS [(a), (c)] and PL spectra [(b), (d)] of the structures with $t_{av} = 0.6$ nm [(a), (b)] and $t_{av} = 1.2$ nm [(c), (d)] of InAs deposited.

electron and hole capture and radiative recombination in QD's. At high excitation densities the drop of luminescence intensity becomes much weaker. Luminescence of the $t_{av} = 0.6$ nm dot shifts at 60–80 K towards smaller photon energies by 50–60 meV. This indicates thermal emission of carriers from smaller InAs QD's to the remaining InAs layer and their efficient subsequent transport into larger dots. At even higher temperatures smaller dots become thermally repopulated.

The relatively broad PL peak stemming from $\sim 10^8$ QD's represents the spectrum R_∞. By using low temperature CL we can excite a much smaller fraction of the dots ($N \sim 30$ dots). The spectrum shows a dramatic change [Fig. 3(a)]; it consists of several ultrasharp lines whose FWHM = 0.15 meV is limited by the spectral resolution of our current setup. The true spectral width is therefore smaller than 0.15 meV, indicating the absence of *inhomogeneous broadening*. The measured carrier lifetime of $\tau = 340$ ps sets a lower limit to FWHM > 0.012 meV. The lines remain that sharp even for elevated temperatures where kT is an order of magnitude larger than the FWHM [Fig. 3(b)]. Thus *thermal broadening* is absent and we have obtained unambiguous spectroscopic evidence for the *zero-dimensional δ-function electronic density of states* in nm-scale single QD's. The remaining background of the spectrum is due to carrier diffusion out of the excitation volume to other dots. At different points of excitation on the sample different peaks evolve due to other slightly different local dot sizes present. For a single QD, containing roughly $(2-3) \times 10^3$ InAs molecules, the theoretical change in confinement energy due to the addition of a single InAs molecule is ~0.06 meV [19]. Thus the minimal detectable line separation corresponds to a change in dot size by only *one single* InAs molecule. The typical separation of the most prominent lines in Fig. 3(a) of ~1 meV corresponds to about 16 InAs molecules.

Monochromatic CL images with spectral resolution $\delta E < 0.3$ meV (see Fig. 4) show that single dots manifest themselves in bright areas about 0.5 μm in radius due to finite carrier diffusion length. Spectra recorded locally in the center of these areas justify this picture since they are dominated by an ultrasharp peak at the detection wavelength due to the particular dot size present. The density of dots having the *same* recombination energy (within the spectral resolution δE) is in the one dot/μm^2 range because the areal density is lowered by the factor $\mathcal{P}(E)\delta E$ which amounts to about 3 orders of magnitude.

In conclusion, we have studied InAs nm-scale QD's in a GaAs matrix. Using highly spatially resolved cathodoluminescence imaging we have shown that each individual dot exhibits one resolution-limited sharp luminescence line (FWHM < 0.15 meV) up to $T = 50$ K, proving for the first time the δ-function density of states. A line sepa-

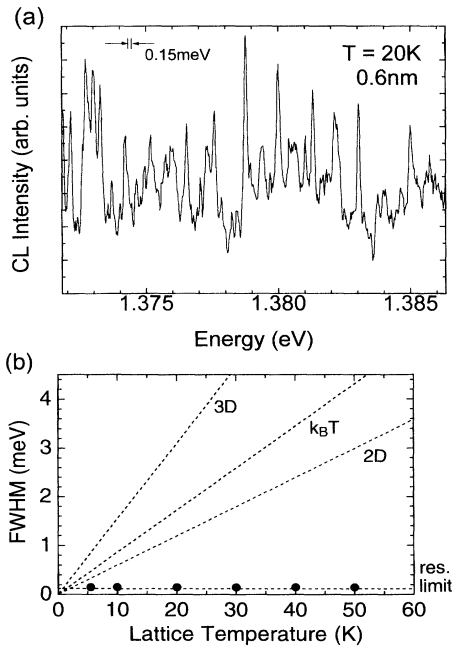

FIG. 3. (a) High spatial resolution ($U = 3$ kV, $I = 60$ pA) CL spectrum of the $t_{av} = 0.6$ nm InAs quantum dots at $T = 20$ K. (b) FWHM of individual dot spectra as a function of temperature. Dashed lines are thermal energy and theoretical half-widths for ideal bulk (3D) and quantum well (2D) material.

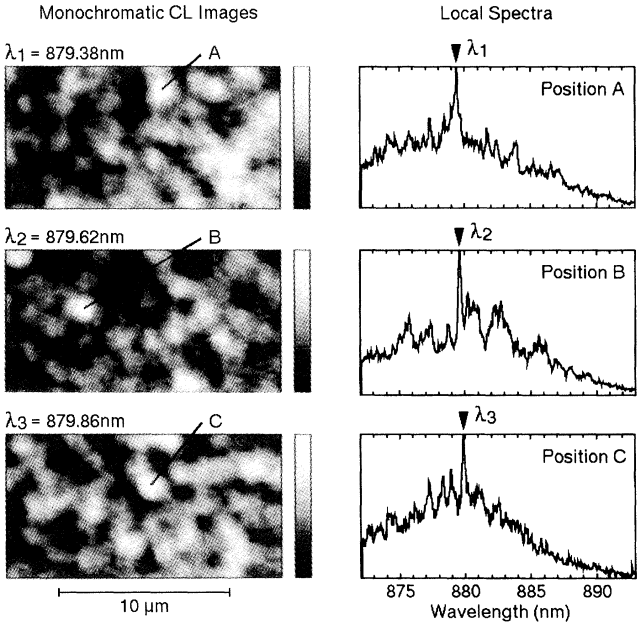

FIG. 4. Low temperature (5 K), monochromatic (spectral resolution <0.2 nm) CL images of $t_{av} = 0.6$ nm InAs quantum dots for three detection wavelengths, differing by 0.38 meV, corresponding to a change in dot size by about six InAs molecules. On the right side are local CL spectra recorded with the electron beam at the positions A, B, and C indicated in the CL images. Arrows on the spectra denote detection wavelength of the CL image to the left.

ration of ~0.06 meV corresponds to a variation of dot size by one single InAs molecule. PL and CAS studies show that the total absorption of the QD ensemble is dramatically increased when a dense array ($\sim 10^{11}$ dots/cm^2) is formed; in this case almost no Stokes shift is observable.

We are indebted to R. Heitz and O. Stier for stimulating discussions. Parts of this work are supported by the Volkswagen Stiftung and by Deutsche Forschungsgemeinschaft in the framework of Grant No. Sfb 296.

Note added.—Zrenner *et al.* [20], Brunner *et al.* [21], and Hess *et al.* [22] observed narrow recombination lines from quantum well excitons localized in potentials caused by interface fluctuations. The existence of such quasi-zero-dimensional systems with small confinement energy was predicted by Christen and Bimberg [23]. Marzin *et al.* [24] have reported a series of sharp lines from small QD ensembles in etched mesas.

*Electronic address: mariusgr@w422zrz.physik.tu-berlin.de World Wide Web: http://sol.physik.tu-berlin.de/

†Permanent address: Otto-von-Guericke Universität, D-39016 Magdeburg, Germany.

‡On leave from A.F. Ioffe Physical-Technical Institute, St. Petersburg, Russia.

§Labor für Elektronenmikroskopie in Naturwissenschaft und Medizin, Weinbergweg, D-06120 Halle/Saale, Germany.

[1] Y. Arakawa and H. Sakaki, Appl. Phys. Lett. **40**, 939 (1982).

[2] H. Sakaki, Surf. Sci. **267**, 623 (1992).

[3] E.L. Ivchenko, A.V. Kavokin, V.P. Kochereshko, P.S. Kop'ev, and N.N. Ledentsov, Superlattices Microstruct. **12**, 317 (1992).

[4] D. Leonard, M. Krishnamurthy, C.M. Reaves, S.P. Denbaars, and P.M. Petroff, Appl. Phys. Lett. **63**, 3203 (1993).

[5] C.M. Reaves, V. Bressler-Hill, M. Krishnamurty, S. Varma, P.M. Petroff, W.H. Weinberg, and S.P. DenBaars, in *Proceedings of the 6th International Conference on InP and Related Materials* (IEEE, Piscataway, 1994), p. 611.

[6] A.I. Ekimov and A.A. Onushenko, JETP Lett. **34**, 345 (1981).

[7] O. Brandt, L. Tapfer, K. Ploog, R. Bierwolf, M. Mohenstein, F. Phillip, H. Lage, and A. Heberle, Phys. Rev. B **44**, 8043 (1991).

[8] R. Nötzel, N.N. Ledentsov, L. Däweritz, M. Hohenstein, and K. Ploog, Phys. Rev. Lett. **67**, 3812 (1991).

[9] J. Tersoff and R.M. Tromp, Phys. Rev. Lett. **70**, 2782–2785 (1993).

[10] Y.M. Mo, D.E. Savage, B.S. Swartzentruber, and M.G. Lagally, Phys. Rev. Lett. **65**, 1020 (1990).

[11] F. Houzay, C. Guille, J.P. Moison, P. Henoc, and F. Barthe, J. Cryst. Growth **81**, 67 (1987); F. Glas, C. Guille, P. Henoc, and F. Houzay, Inst. Phys. Conf. Ser. **87**, 71 (1987); J.M. Moison, F. Houzay, F. Barthe, L. Leprince, E. Andre, and O. Vatel, Appl. Phys. Lett. **64**, 196 (1994).

[12] R. Nötzel, J. Temmyo, and T. Tamamura, Jpn. J. Appl. Phys. **33**, L275 (1994).

[13] N.N. Ledentsov, A.Yu. Egorov, A.E. Zhukov, M.V. Maksimov, I.G. Tabatadze, and P.S. Kop'ev, Fiz. Tekh. Poluprovodn. **28**, 343 (1994); [Semiconductors **28**, 832 (1994)].

[14] J. Christen, M. Grundmann, and D. Bimberg, J. Vac. Sci. Technol. B **9**, 2358 (1991).

[15] D. Bimberg, T. Wolf, and J. Böhrer, in *Advances in Nonradiative Processes in Solids,* edited by B. di Bartolo (Plenum, New York, 1991), p. 577.

[16] P.D. Wang, N.N. Ledentsov, C.M. Sotomayor Torres, P.S. Kop'ev, and V.M. Ustinov, Appl. Phys. Lett. **64**, 1527 (1994).

[17] A. Ksendzov, F.J. Grunthaner, J.L. Liu, D.H. Rich, R.W. Terhune, and B.A. Wilson, Phys. Rev. B **43**, 14574 (1991).

[18] R. Heitz (unpublished).

[19] Details about our three-dimensional strain simulation and band structure calculations will be presented elsewhere.

[20] A. Zrenner, L.V. Butov, M. Hagn, G. Abstreiter, G. Böhm, and G. Weimann, Phys. Rev. Lett. **72**, 3382 (1994).

[21] K. Brunner, G. Abstreiter, G. Böhm, G. Tränkle, and G. Wiemann, Appl. Phys. Lett. **64**, 3320 (1994).

[22] H.F. Hess, E. Betzig, T.D. Harris, L.N. Pfeiffer, and K.W. West, Science **264**, 1740 (1994).

[23] J. Christen and D. Bimberg, Phys. Rev. B **42**, 7213 (1990), Fig. 4.

[24] J.-Y. Marzin, J.-M. Gérard, A. Izraël, D. Barrier, and G. Bastard, Phys. Rev. Lett. **73**, 716 (1994).

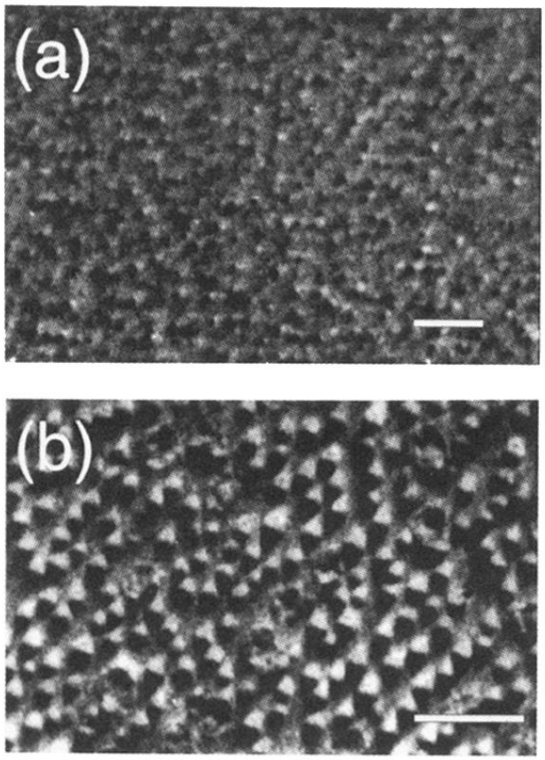

FIG. 1. Plan-view TEM images of InAs quantum dots in a GaAs matrix. Average thickness of InAs deposited is (a) $t_{av} = 0.6$ nm and (b) $t_{av} = 1.2$ nm. Markers represent 100 nm.

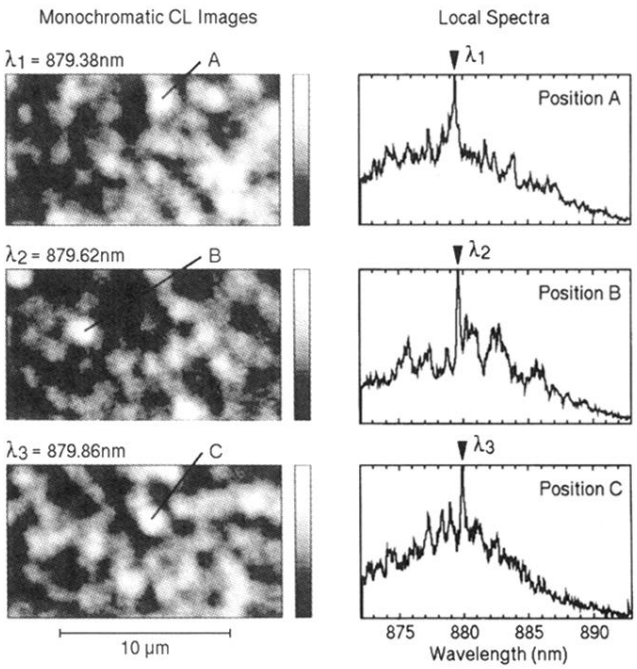

FIG. 4. Low temperature (5 K), monochromatic (spectral resolution <0.2 nm) CL images of t_{av} = 0.6 nm InAs quantum dots for three detection wavelengths, differing by 0.38 meV, corresponding to a change in dot size by about six InAs molecules. On the right side are local CL spectra recorded with the electron beam at the positions A, B, and C indicated in the CL images. Arrows on the spectra denote detection wavelength of the CL image to the left.